EARTHQUAKE PERFORMANCE OF CEVİZLİBAĞ METROBUS OVERPASS

Emrullah Dar

Boğaziçi University Kandilli Observatory

And Earthquake Research Institute

Earthquake Engineering Department

TOMORROW'S CITIES TECHNICAL REPORT

March 2020

Tomorrow's Cities is the UKRI GCRF Urban Disaster Risk Hub

About **Tomorrow's Cities**

"Our mission is to reduce disaster risk for the poor in tomorrow's cities."

Tomorrow's Cities is the UK Research and Innovation (UKRI) Global Challenges Research Fund (GCRF) Urban Disaster Risk Hub – a five-year global interdisciplinary research hub.

Our aim is to catalyse a transition from crisis management to multi-hazard risk-informed and inclusive planning and decision-making, for cities in low-and-middle income countries.

Globally, more than two billion people living in cities of low-to-middle income countries are exposed to multiple hazards such as floods, earthquakes, landslides, volcanoes and fires, which threaten the cyclical destruction of their lives and livelihoods. With urban areas expanding at unprecedented rates, this number is expected to reach four billion by 2050.

Failure to integrate multi-hazard disaster risk into urban planning and decision-making presents a major barrier to sustainable development, including the single greatest global challenge of eradicating poverty in all its forms.

But this global challenge is also major opportunity: as ~60% of the area expected to be urban by 2030 remains to be built, we can reduce disaster risk in tomorrow's cities by design.

We are one of 12 UKRI GCRF Hubs funded by a UKRI Collective Fund Award, as part of the UK AID strategy, putting research at the heart of efforts to deliver the United Nation's Sustainable Development Goals (SDGs).

www.tomorrowscities.org
@UrbanRiskHub
The UKRI GCRF Urban Disaster Risk Hub
ECCI High School Yards, Infirmary Street, Edinburgh EH1 1LZ

CONTENTS

1. Introduction

This report is a sub-run of the work package 2.6 of the Tomorrow Cities project called "Multi-hazard Physical Vulnerability of Transport Infrastructure". Within the scope of this study, the multi-hazard risk of the two overpasses selected in Istanbul is investigated. These overpasses are the Cevizlibağ and Incirli Metrobus Overpasses, which are located on the highway with the highest traffic density in Istanbul and where the pedestrian density is quite high. In this report, only the Cevizlibağ Overpass is discussed, and earthquake performance is investigated.

Cevizlibağ Metrobus Overpass was built in 2007 for pedestrians to reach Cevizlibağ Metrobus Station which is located at Zeytinburnu District (Figure 1). This overpass was expanded in 2013 due to insufficient pedestrian access because of increased pedestrian density. In 2017, the aging parts of the overpass were renewed and polyurethane-based waterproofing was applied to the walkway and stairs to prevent it from rusting[1] According to 2013 data, the overpass is used by 35 thousand people daily[2]. The length of the bridge is 122 m, its width is 5.9 m, and its ground clearance is 5 m.

Cevizlibağ Metrobus Overpass has a very important place in Istanbul transportation due to its high pedestrian density and its location on the main road with heavy vehicle traffic. Damage to the Cevizlibağ overpass in a possible earthquake may block the traffic of Istanbul and prevent the aid teams from reaching the earthquake victims. If it collapses in an earthquake while the density of people is high on it, it may cause many casualties. For this reason, this overpass should be designed in such a way that it will not be damaged even in the biggest possible earthquake. Also, there are 4 stairs on the overpass and a platform with turnstiles for Metrobus passes (Figure 2).

This study aims to determine the dynamic (Modal parameters such as modal frequencies and mode shapes) and static properties (Geometry and material properties) of the Cevizlibağ Overpass and to examine the earthquake performance. In this context, the building was analyzed under the earthquake levels defined in the 2018 Turkish Earthquake Code. As a result of these analyzes, the total shear force capacity of the structure and the amount of shear force demanded from the structure were calculated using different earthquake levels.

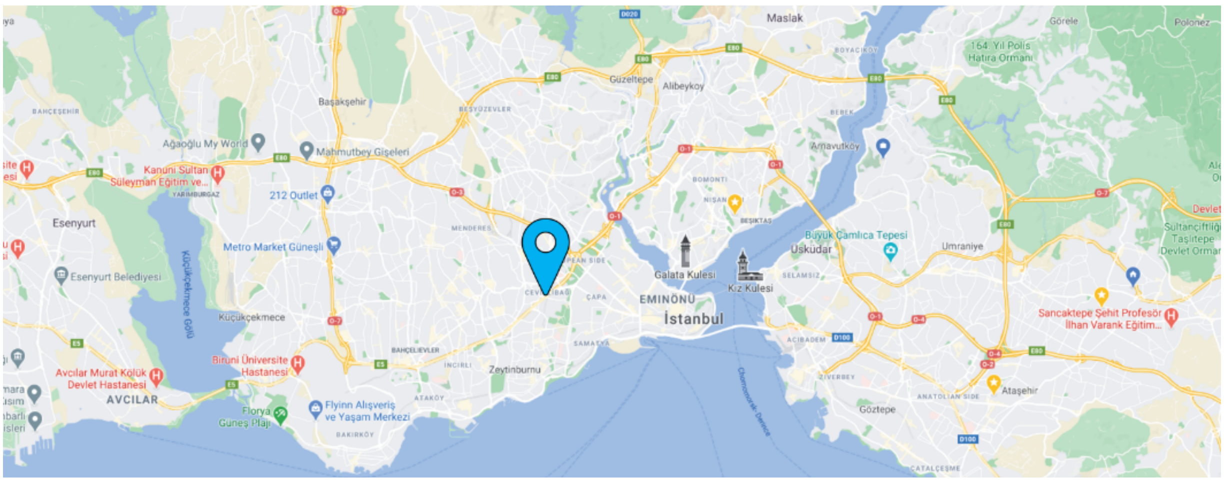

Figure 1. The location of Cevizlibağ Metrobüs Overpass in Istanbul Map.

Figure 2. The view of Cevizlibağ Metrobüs Overpass.

To determine the dynamic parameters of the overpass, vibration measurements were carried out on 11.02.2020 between 05:45 and 08:45 with three accelerometers. In order to evaluate the conditions where the pedestrian density is low and high in the Overpass, the measurement started in the early hours of the morning and continued until the rush hours. Two of these accelerometers are located at both ends of the overpass and one on the ground. Accelerometers operated at 100 Hz and low-frequency waves were eliminated by applying a 0.2 Hz high-pass filter to all recordings. The layout and directions of the accelerometers are shown in Figure 3.

Figure 3. The layout and directions of the accelerometers are shown in Figure 3.

2. Modal Identification of the Overpass

According to the records obtained from accelerometers, vibrations on the ground increase as pedestrian density increases (Figure 4). As expected, as the pedestrian density increased, the vibrations in the vertical direction increased more than the vibrations in the horizontal direction. The rate of increase of the average acceleration in the horizontal and vertical direction is between 30-50% and 60-80%, respectively. The increase in acceleration and velocity records is greater than the increase in displacement.

As pedestrian density increased, accelerations at Station A increased by 400-500%, and accelerations at Station B increased by 300-400%. At Station A, the maximum acceleration is approximately 11 cm/s^2 in the East-West direction, 7 cm/s^2 in the North-South direction, and 19 cm/S^2 in the vertical direction (Figure 5). At Station B, the maximum acceleration is approximately 7 cm/s^2 in the East-West direction, 5 cm/s^2 in the North-South direction, and 9 cm/S^2 in the vertical direction (Figure 6).

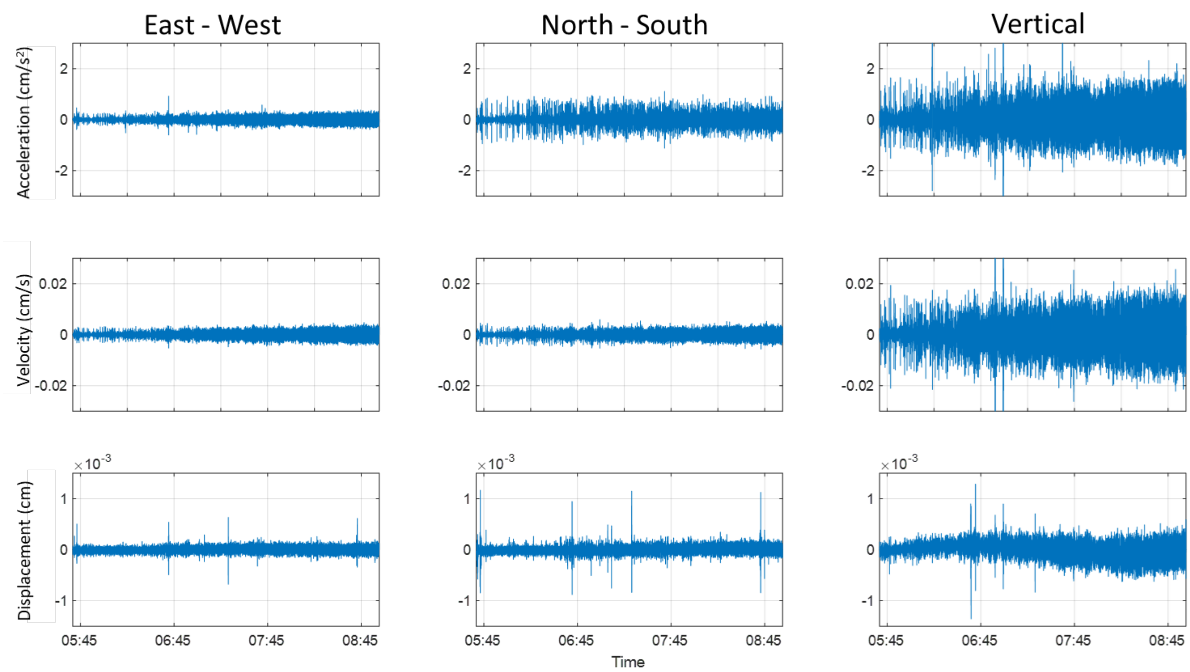

Figure 4. Three-dimensional acceleration, velocity, and displacement records at Ground Station.

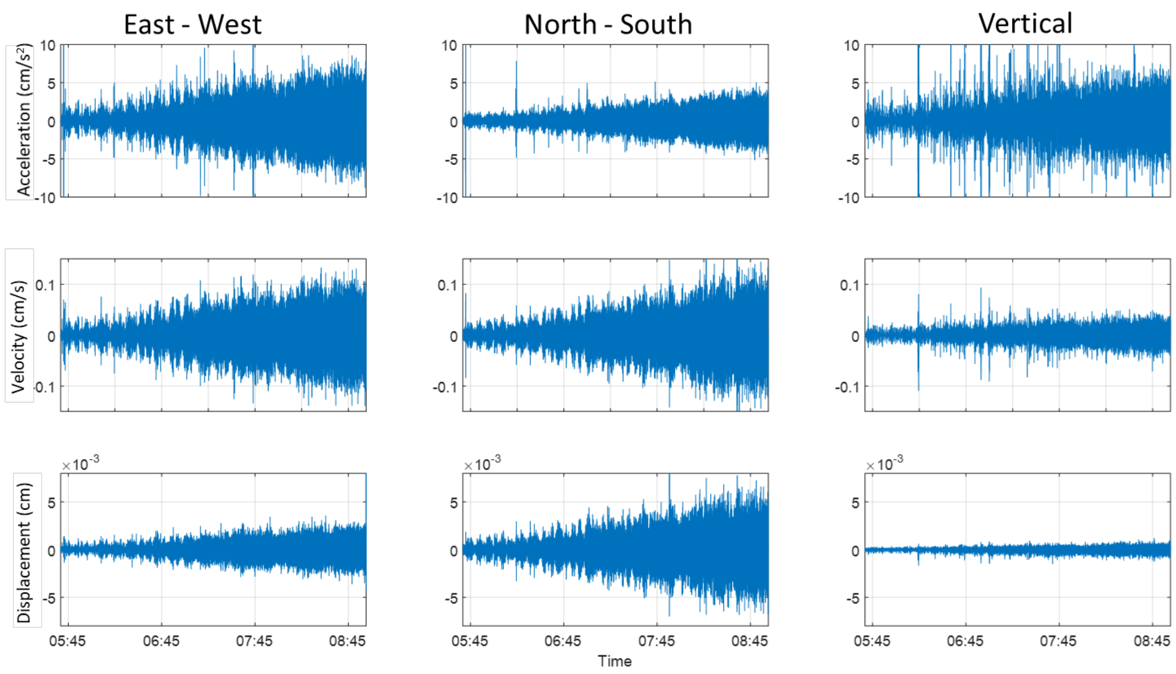

Figure 5. Three-dimensional acceleration, velocity, and displacement records at A Station.

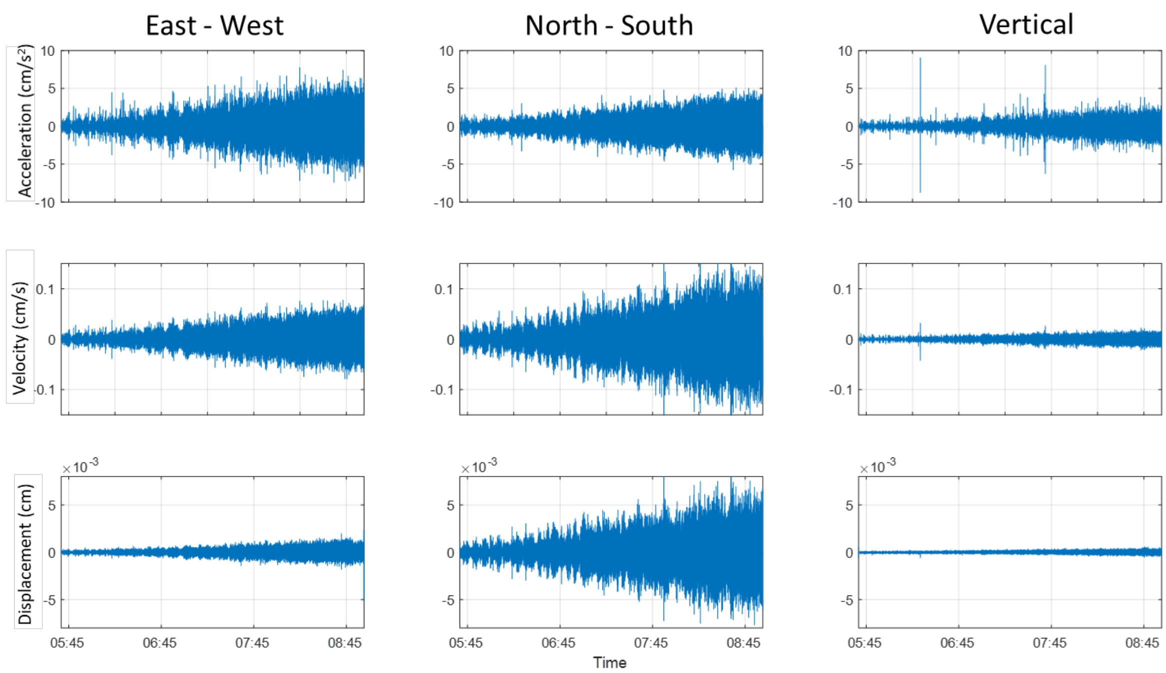

Figure 6. Three-dimensional acceleration, velocity, and displacement records at B Station.

In order to determine the modal frequencies of the overpass, the records were examined at the frequency base. For this purpose, Fourier amplitude spectrums (FAS) of the records were calculated. To understand the dynamic behavior of the structure in the loaded and unloaded case, the records were examined in two parts, between 5: 45-6: 00 and 8: 30-8: 45. The modal frequencies of the structure are determined by using transfer functions to eliminate the ground effect. The formulation of the transfer function is as follows:

$$H(f) = \frac{Y(f)}{X(f)}$$

In this formulation, H (f) represents the transfer function, Y (f) represents FAS of Station A and Station B and X (f) represents FAS of the ground station.

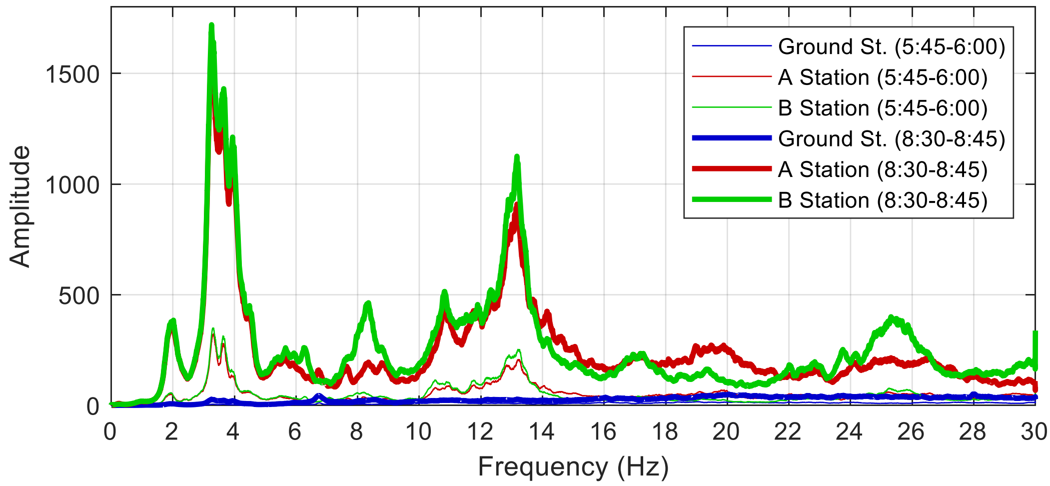

Figure 7. Fourier Amplitude Spectra of stations on North-South direction for hours of low and high pedestrian density.

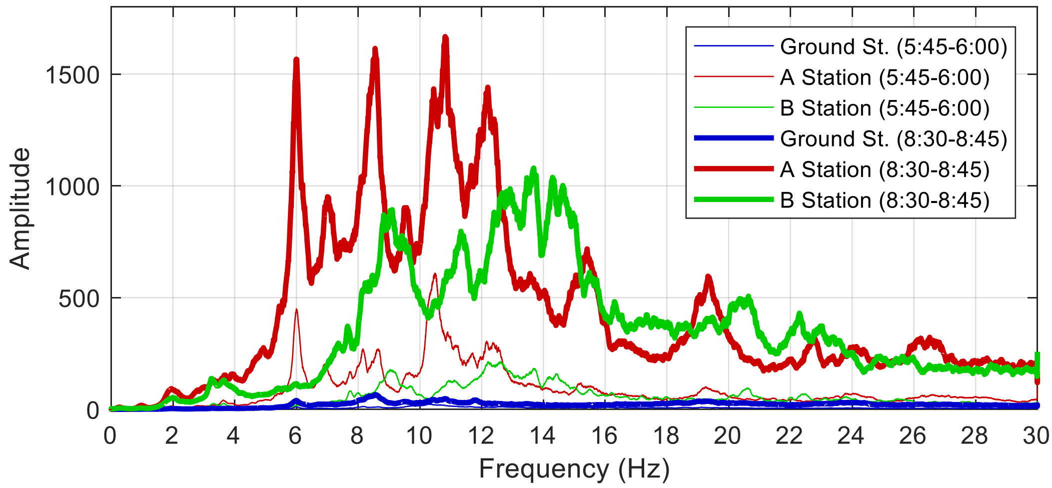

Figure 8. Fourier Amplitude Spectra of stations on East-West direction for hours of low and high pedestrian density.

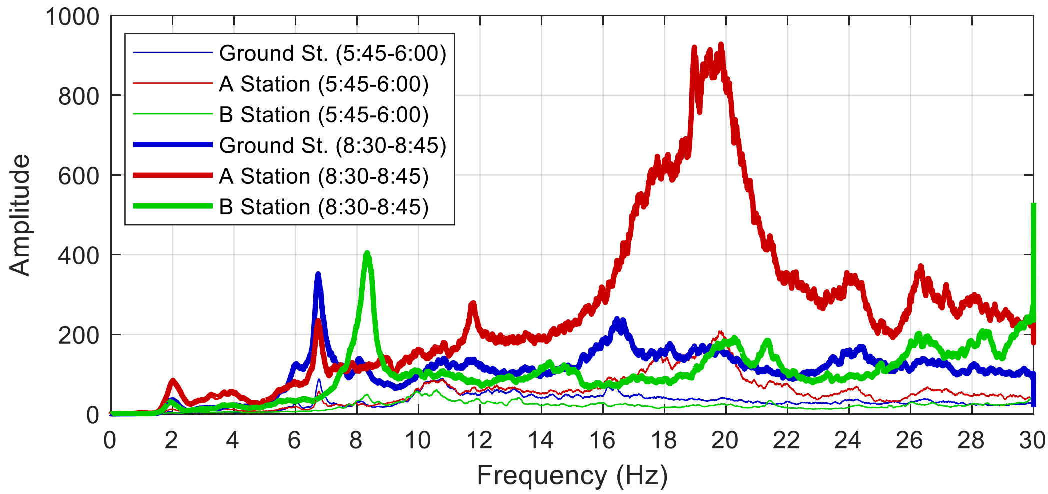

Figure 9. Fourier Amplitude Spectra of stations in the vertical direction for hours of low and high pedestrian density.

According to the results, the transfer functions of stations A and B in the North-South direction are almost identical. This is because the North-South direction is the longitudinal direction of the overpass and in this direction, the deck of the overpass works as a diaphragm. At the same time, this result shows that there is no gap in the deck and it can transfer load.

The first mode shape of the structure is a linear motion in the N-S direction in the range of 3.22-3.34 Hz. (Figure 7). The second mode is linear in the E-W direction in the range of 5.9 - 6.1 Hz, but station A is more mobile than station B (Figure 8). The third mode is the torsional mode in the range of 8.2-8.4 Hz. All obtained modal frequencies are shown in Table 1.

Table 1. Modal frequencies estimated via transfer functions.

	Mode 1 (Hz)	**Mode 2 (Hz)**	**Mode 3 (Hz)**
Station A (N-S)	3.22-3.34	8.2-8.4	13-13.2
Station B (N-S)	3.22-3.34	8.2-8.4	13-13.2
Station A (E-W)	5.9-6.1	8.2-8.4	10.5-10.9
Station B (E-W)	8.9-9.1	11.4-11.6	13.8-14

There is a high amplitude vibration around 19 Hz in the vertical direction at the ground station. (Figure 9). This vibration may be caused by vehicle or pedestrian traffic. As the pedestrian density increased, the amplitudes of the frequencies increased approximately 4 times in the East-West direction and approximately 5 times in the North-South direction and the vertical direction. However, a limited decrease in modal frequencies was observed. The first modal frequency has temporarily decreased from 3.34 Hz to 3.22 Hz with the increase in pedestrian density. (Figure 10).

In order to investigate the effect of pedestrian movements on the modal shape of the overpass, the modal shapes of the building were calculated for every 10 minutes of data. Mode shapes can be calculated in many different ways. The most common method used for the identification of mode shapes is the Frequency Domain Decomposition (FDD) method. This method can be defined as Singular Value Decomposition (SVD) of Cross-Power Density Function (CPDF), which is formulated as

$$SVD(P_{xy})_{m\times m} = U_{m\times m}\,\Sigma_{m\times n}\,V_{n\times n}$$

Where $U_{m\times m}$ is the mode Shape Matrix and $\sum_{m\times n}$ is the mode amplitudes. There are many methods for calculating the change of the specified mode shape. Among these methods, the MAC is the most widely used and obtained as

$$MAC(n) = \frac{|\{\Phi_r\}^T\{\Phi_n\}|^2}{|\{\Phi_r\}^T\{\Phi_r\}||\{\Phi_n\}^T\{\Phi_n\}|}$$

where$\{\Phi_r\}$ is the reference mode shape and $\{\Phi_n\}$ is the mode shape at the n^{th} window. The mode shape estimated in the time window between 05:30 and 05:40 am is assumed to be the reference mode shape. By comparing mode shapes estimated in the following windows with the reference mode shape, mode shape variations could be tracked. The first mode shape changes calculated using the MAC method are shown in Figure 11. In light of these results, it can be said that the bridge maintained its mode shape until 07:00 am, but after that, the mode shape changed temporarily with increased pedestrian density.

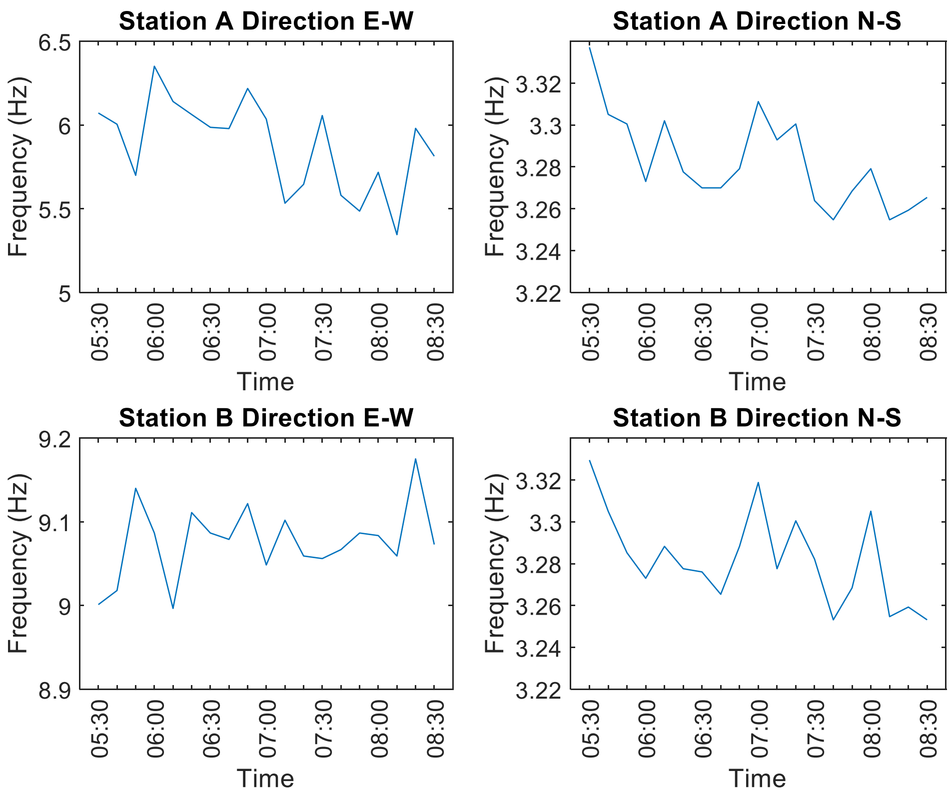

Figure 10. Modal frequency variations between 05:30 and 08:30.

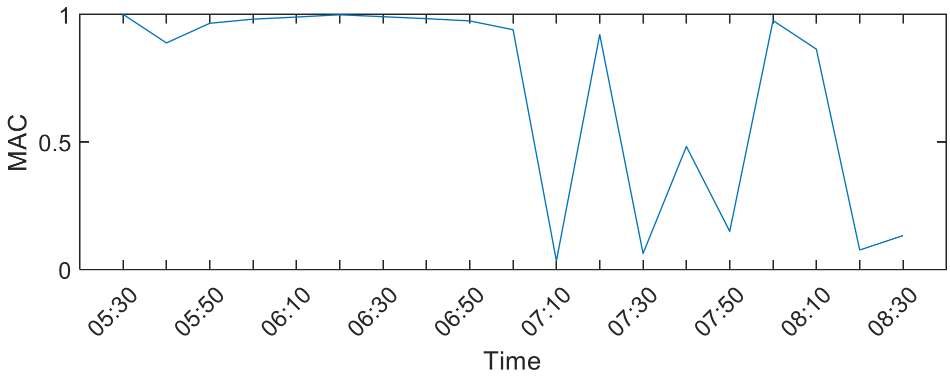

Figure 11. The variation of first mode shape between 05:30 and 08:30.

3. Modeling

3.1 The Summary of the model

The modeled overpass is a steel bridge with 9 spans and double columns on each support. It is carried by 20 columns, which are 5 meters in height and are Y-shaped. Since we could not reach the static and architectural projects of the bridge, all measurements were taken with laser meters in the field. As material properties, material properties on similar overpasses built on the same dates were used. Therefore, we do not have enough data to perform a detailed analysis of all elements. For this reason, the total shear force and total shear force capacities were calculated in this model and the structure was evaluated in the light of these two data. For this reason, in this model, the total shear force that can affect the structure under different earthquake scenarios and the total shear force capacity of the structure is calculated. The general condition of the building was interpreted by evaluating these two data.

The total length of the overpass is about 120 meters. It has a total of 4 stairs and a passenger crossing platform. In this study, stairs and the platform are neglected to simplify the model. The size of the columns is 30x70 cm at the base and expands upwards by taking the Y shape. The distance between adjacent columns is 2.15 m and the width of the deck is 5.9 m. There are three 20x30 cm continuous beams on the columns. There are three continuous main beams with dimensions of 20x36 cm on the columns. The wall thickness of steel in columns and beams is considered to be 16 mm. As a steel grade, S355 Steel is used in the model. The three-dimensional view of the model is shown in Figure 12.

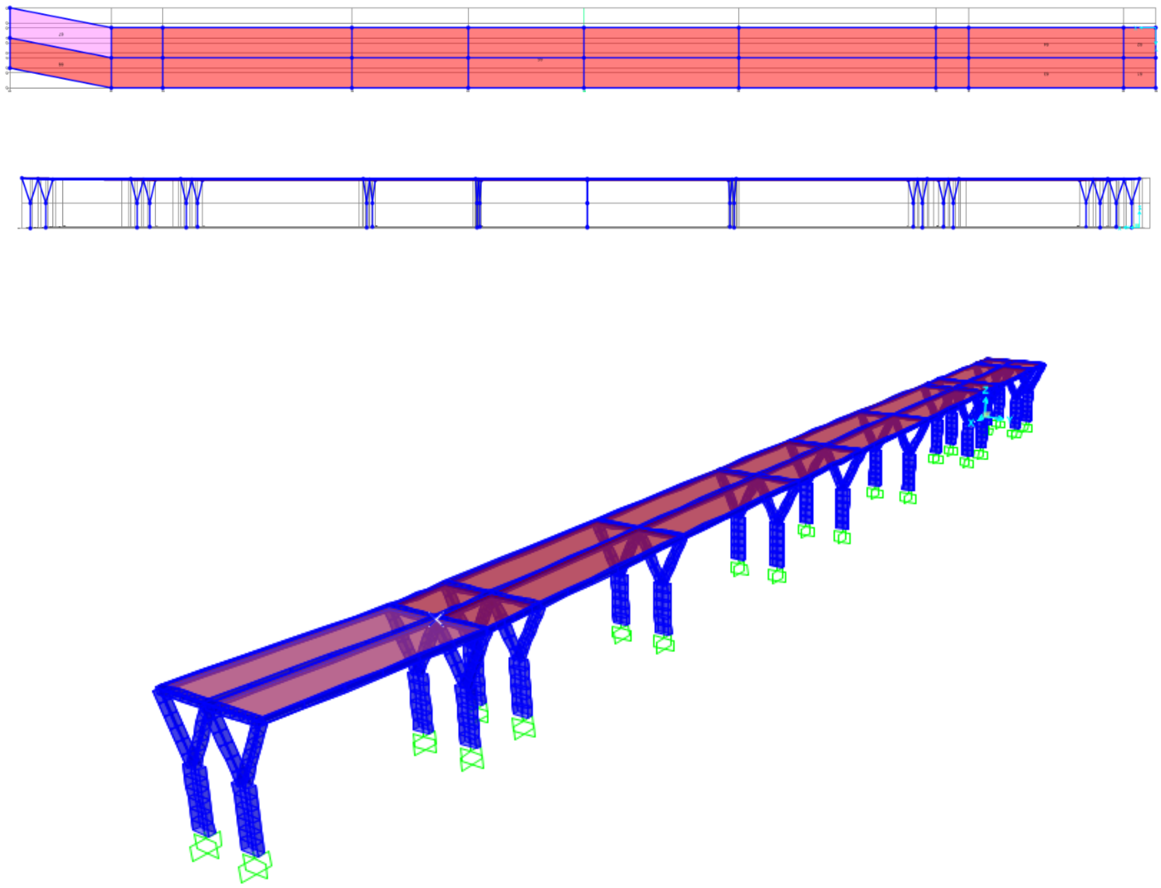

Figure 12. Three-dimensional view of the overpass model.

3.1 Total Mass Calculation

To calculate the total shear force, it is necessary to calculate the total weight of the structure. But since we do not have projects for the bridge, the total weight is also calculated as an estimate. The estimated weights of the columns, main beams, small beams, deck, stairs, pedestrian platform, and railings are calculated and summed. Table 2 shows the estimated weights of the elements of the bridge. According to these results, the empty weight of the bridge was calculated as approximately 278 tons.

Table 2. The estimated weights of the elements of the bridge

Structural Element	**Ton**
Columns	100-110
Main Beams	35-40
Minor Beams	13-15
Deck	70-80
Stairs+Platform	30-35
Railing	13-15
Total	**261-295**
	≈278

In the live load calculation, the pedestrian capacity of the bridge is taken into consideration. In the observations made, it was determined that there is a maximum of 240 pedestrians on the overpass during the hours when the pedestrian density was the highest. If we calculate the average weight of each pedestrian as 80 kg, the live load is obtained as approximately 19 tons. According to the 2018 Turkish Earthquake Code, the total weight of the building is obtained by multiplying the dead loads 1.4 and the live loads 1.6. In this case, the total building weight is as follows:

$$\text{Unloaded case: } 1.4 \times 278 + 1.6 \times 0 = 390 \text{ ton}$$

$$\text{Loaded Case: } 1.4 \times 278 + 1.6 \times 19 = 420 \text{ ton}$$

3.2 Applied excitation and analysis details

The modeled bridge was analyzed according to the equivalent earthquake load method specified in the Turkish Earthquake Regulation (2018). Spectral accelerations of the bridge are obtained by elastic design Spectra calculated for four different earthquake levels defined in the Code. The descriptions of earthquake levels defined in the code are given in Table 2. The short-period design spectral acceleration coefficients (S_{DS}) and the 1 second period design spectral acceleration coefficients (S_{D1}) are taken from an interactive web application prepared by the Turkish Disaster and Emergency Management Directorate (AFAD)[3] according to site class, earthquake level, and location of the structure. The site class of the building is selected as "Site Class C" from the ground classification map prepared by the Istanbul Metropolitan Municipality in 2007[4]. Using S_{DS} and S_{D1} coefficients, T_A and T_B values, which are corner periods of the spectrum, were obtained by the following formula:

$$T_A = 0.2\frac{S_{D1}}{S_{DS}} \ , \qquad T_B = \frac{S_{D1}}{S_{DS}}$$

The resulting spectral parameters are shown in table 4. Spectral accelerations were calculated as follows:

$$S_a(T) = \left(0.4 + 0.6\frac{T}{T_A}\right)S_{DS} \qquad 0 \le T \le T_A$$

$$S_a(T) = S_{DS} \qquad T_A \le T \le T_B$$

$$S_a(T) = \frac{S_{DS}}{T} \qquad T_B \le T \le 6\ s$$

Table 3. The definitions of Earthquake levels according to the Turkish Earthquake Code 2018.

Earthquake Level	Definition
DD-1 Earthquake	The earthquake has a return period of 2475 years.
DD-2 Earthquake	The earthquake has a return period of 475 years.
DD-3 Earthquake	The earthquake has a return period of 72 years.
DD-4 Earthquake	The earthquake has a return period of 43 years.

Table 4. Response spectrum parameters of the bridge.

Earthquake Level	PGA (g)	PGV (cm/sn)	S_{D1}	S_{DS}	T_A	T_B
DD-1	0.688	43.3	0.882	1.733	0.102	0.509
DD-2	0.409	25.1	0.565	1.096	0.103	0.515
DD-3	0.167	10.24	0.253	0.576	0.088	0.439
DD-4	0.108	6.5	0.161	0.398	0.081	0.0404

The response spectrum obtained according to the Turkish Earthquake Regulation is shown in Figure 13. According to these results, the period of the structure remains within the peak plateau region of the spectrum. Therefore, it can be expected that the structure will be exposed to maximum spectral acceleration in possible earthquakes. The total shear force for each earthquake level is calculated according to the following formula specified in the code:

$$V_t = M_t S_a(T) \geq 0.04\, m_t I S_{DS}\, g$$

The total shear force calculated of the deck according to this formulation and maximum horizontal displacement is shown in Table 5 and Table 6, respectively, for unloaded and loaded conditions.

Table 5. Total shear force for four earthquake levels and displacements for the unloaded case.

	Sae(g)	*Mt*	*Vte(g)*	*Vte(t)*	*D(mm)*
DD-1	1,733	390	675,87	6630,285	36,1
DD-2	1,096	390	427,44	4193,186	22,81
DD-3	0,576	390	224,64	2203,718	11,97
DD-4	0,398	390	155,22	1522,708	8,27

Table 6. Total shear force for four earthquake levels and displacements for the loaded case.

	Sae(g)	*Mt*	*Vte(g)*	*Vte(t)*	*D(mm)*
DD-1	1,733	420	727,86	7140,307	36,1
DD-2	1,096	420	460,32	4515,739	22,81
DD-3	0,576	420	241,92	2373,235	11,97
DD-4	0,398	420	167,16	1639,84	8,27

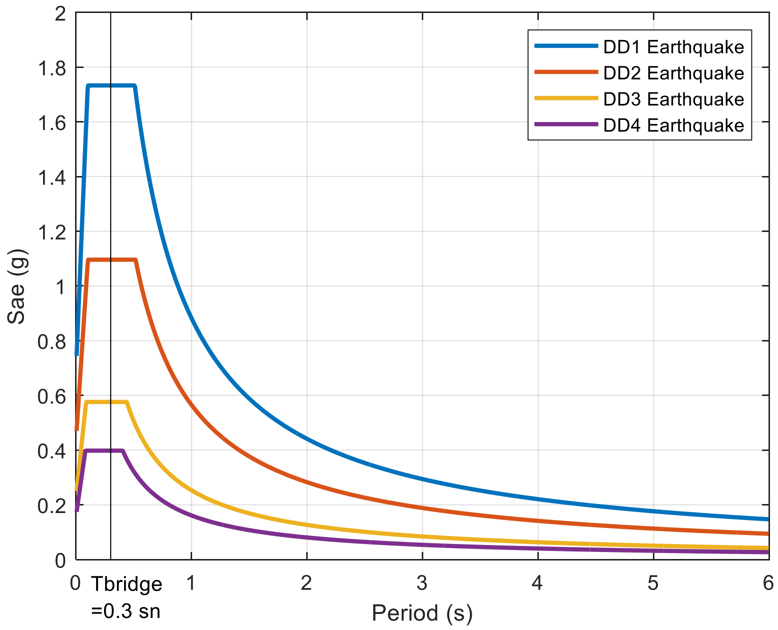

Figure 13. Response spectra of the bridge for four earthquake levels.

4. Results

As a result of the numerical analysis performed, the shear forces calculated for each column are shown in Table 7 and Table 8 for unloaded and loaded cases respectively. For both loaded and unloaded cases, the bridge will show elastic behavior in DD-2, DD-3, and DD-4 earthquakes, and no plastic deformation is expected. But in a DD-1 earthquake, the shear force acting on the bridge slightly exceeds the shear force capacity of the bridge for each case. This, in turn, shows that the structure will show some plastic behavior in this earthquake. The damage will remain fairly limited, and severe damage or complete collapse is not expected for the unloaded case. However, in the loaded case, the demanded shear force reaches 10-15% above the shear force capacity of the structure. This can cause severe damage to the overpass. However, in both cases, complete collapse is not expected.

Table 7. The total amount of shear force acting on the columns in the no-load case.

	DD-1	*DD-2*	*DD-3*	*DD-4*
Column No	**Stress (N/mm2)**	**Stress (N/mm2)**	**Stress (N/mm2)**	**Stress (N/mm2)**
1	346.959	219.269	117.329	79.544
2	383.750	242.521	129.591	87.979
3	364.139	230.127	123.045	83.483
4	383.242	242.200	129.407	87.862
5	343.703	217.212	116.231	78.798
6	384.961	243.286	129.991	88.257
7	346.257	218.826	117.091	79.383
8	384.462	242.971	129.808	88.142
9	343.736	217.233	116.238	78.805
10	385.317	243.511	130.096	88.338
11	345.308	218.226	116.765	79.166
12	369.153	233.295	124.714	84.632
13	331.885	209.743	112.294	76.088
14	379.624	239.913	128.203	87.033
15	340.795	215.374	115.264	78.131
16	383.428	242.317	129.454	87.905
17	336.289	212.526	113.747	77.098
18	389.117	245.912	131.355	89.209
19	345.280	218.209	116.749	79.159
20	394.391	249.246	133.116	90.418
21	352.642	222.861	119.206	80.847
22	327.202	206.784	110.735	75.015

Table 8. The total amount of shear force acting on the columns in the loaded case.

	DD-1	DD-2	DD-3	DD-4
KOLON	**Stress (N/mm2)**	**Stress (N/mm2)**	**Stress (N/mm2)**	**Stress (N/mm2)**
1	373.675	236.153	126.363	85.669
2	413.299	261.195	139.570	94.753
3	392.178	247.847	132.519	89.911
4	412.752	260.849	139.371	94.627
5	370.168	233.937	125.181	84.865
6	414.603	262.019	140.000	95.053
7	372.919	235.676	126.107	85.495
8	414.066	261.680	139.803	94.929
9	370.204	233.960	125.188	84.873
10	414.986	262.261	140.113	95.140
11	371.897	235.029	125.756	85.262
12	397.578	251.259	134.317	91.149
13	357.440	225.893	120.941	81.947
14	408.855	258.386	138.075	93.735
15	367.036	231.958	124.139	84.147
16	412.952	260.975	139.422	94.674
17	362.183	228.891	122.506	83.035
18	419.079	264.847	141.469	96.078
19	371.867	235.011	125.739	85.254
20	424.759	268.438	143.366	97.380
21	379.795	240.021	128.385	87.072
22	352.397	222.706	119.262	80.791

5. Conclusion

In this study, Cevizlibağ Metrobus Overpass is evaluated in terms of earthquake performance. Since the measurements obtained in the field about the overpass are not sufficient for detailed performance analysis, it was preferred to calculate the total shear force and capacity of the columns. The results are summarized below:

- The modal vibration frequency of the overpass is affected to a limited extent by the pedestrian intensity, but the mode shape varies greatly accordingly.
- It is expected that the DD-2, DD-3, and DD-4 earthquakes will not cause permanent plastic deformation on the overpass.
- A limited degree of plastic deformation is expected in the no-load case in the DD-1 earthquake. However, plastic deformation is expected in all columns, as the total shear force in the loaded case will exceed 10-15% of the shear force capacity of the structure.
- Although plastic deformations in the structure are expected in the DD-1 earthquake in both load cases, complete collapse is not expected.

Considering the location of the cevizlibağ overpass and heavy pedestrian and vehicle traffic, even limited damage to the overpass can negatively affect all Istanbul traffic. For this reason, it is necessary to examine the earthquake performance of this overpass with more detailed data and take the necessary precautions against possible damage.

References

1. Website: https://www.ibb.istanbul/News/Detail/34177).
2. Website: https://www.haberler.com/cevizlibag-metrobus-istasyonu-genisletiliyor-4844034-haberi/
3. Website: https://www.turkiye.gov.tr/afad-turkiye-deprem-tehlike-haritalari
4. Website:http://ibb.gov.tr/trTR/SubSites/DepremSite/Documents/EK16_Zemin_Siniflamasi_Haritasi_1440x910_25000_300DPI.pdf